

RSC Advances



This is an *Accepted Manuscript*, which has been through the Royal Society of Chemistry peer review process and has been accepted for publication.

Accepted Manuscripts are published online shortly after acceptance, before technical editing, formatting and proof reading. Using this free service, authors can make their results available to the community, in citable form, before we publish the edited article. This *Accepted Manuscript* will be replaced by the edited, formatted and paginated article as soon as this is available.

You can find more information about *Accepted Manuscripts* in the [Information for Authors](#).

Please note that technical editing may introduce minor changes to the text and/or graphics, which may alter content. The journal's standard [Terms & Conditions](#) and the [Ethical guidelines](#) still apply. In no event shall the Royal Society of Chemistry be held responsible for any errors or omissions in this *Accepted Manuscript* or any consequences arising from the use of any information it contains.

Cite this: DOI: 10.1039/c0xx00000x

www.rsc.org/xxxxxx

ARTICLE TYPE

Introduction of 'lattice-voids' in high tap density TiO₂-B nanowires for enhanced high-rate and high volumetric capacity lithium storageZhong Su^a, Yuxuan Zhu^a, Zhenzhen Wu^a, Xiaoyu Peng^b, Chenlong Gao^b, Kai Xi^{*b}, Chao Lai^{*a,b}, R. Vasant Kumar^b*Received (in XXX, XXX) Xth XXXXXXXXX 20XX, Accepted Xth XXXXXXXXX 20XX*

DOI: 10.1039/b000000x

TiO₂-B nanowires with a high tap density, containing structural lattice voids within each nanowire, is prepared via a tailored hydrothermal-calcination route. These internal voids, formed by controlling the calcination temperature as clusters of vacant sites enable fast transport of lithium-ions within the lattice material, leading to enhanced high-rate performance of TiO₂-B nanowire based electrode in a Li-ion battery. At a current density of 2000 mA g⁻¹, a high value of discharge capacity at 129.0 mAh g⁻¹ is retained after 80 cycles. Our results indicate that electrode based on this nanowire material with 'lattice-voids' structure and high tap density, meets the challenge of achieving a high-rate performance and a high volumetric density in Li-ion batteries.

Introduction

Safety of lithium-ion batteries is one of the primary concerns in their practical application, especially for utilizations in electric vehicles and hybrid electric vehicles.¹⁻³ In the past two decades, many safer alternatives to commercially used graphite anode have been investigated, and titania-based anode materials are of particular interest, due to their lower cost, environmental friendliness, and particularly their higher lithium intercalation potential such that the dendrite deposition of metallic lithium is avoided.⁴ TiO₂ has been suggested as a suitable anodic host, with most attention paid to the tetragonal metastable anatase form. TiO₂ can offer a higher theoretical capacity (335 mAh g⁻¹, assuming one Li atom per TiO₂ unit) than other contenders such as Li₄Ti₅O₁₂. TiO₂-B is another metastable phase of titanium dioxide, which has been seriously considered as an ideal host for Li⁺ intercalation compared to anatase or rutile TiO₂.⁵⁻¹⁰ Hence TiO₂-B anode materials are receiving increasing attention, and nanostructured TiO₂-B, such as nanotubes, nanowires and nanoparticles, have been widely investigated as high-performance anode materials.⁵⁻¹⁰ Typically 1-D nanotubes can offer mesoporous ordering and good electrode-electrolyte contact to produce excellent rate performance, but also an inferior packing and highly irreversible initial capacity. Following the demand of practical applications, an important challenge is to provide a suitable 1-D nanostructured electrode offering a high tap density and a high-rate discharge capability.^{8,9} As compared to nanotubes, TiO₂-B nanowires at a lower surface area can offer a higher tap

density, but suffers from a poorer high-rate discharge capability.^{8,9} Thus, achievement of vastly improved rate performance with TiO₂-B nanowires will be considered to be a significant progress.

When TiO₂-B, is used in the form of high surface area nanowires with very small diameter (7-15nm) in order to facilitate favorable electronic and ionic transport, good rate performance is achievable.¹⁰ Deliberate introduction of hierarchical pores and thus achieving a high surface area in the anode made up of nanowires, is a productive avenue as the nanopores can help further shorten the transport distance of lithium-ions and electrons.⁶ However, similar to nanotubes, such modifications will result in poorer tap density from inferior packing, thus placing an important volumetric limit in their potential practical application. Another possible strategy is to modify the crystal structure of the TiO₂-B material, for example, by producing the disordered structure in the lattice itself such that the ionic transport is enhanced. The generation of partial disordered structure in the crystalline TiO₂-B nanowires can further enhance the lithium-ion diffusion coefficient in the anode structure, without the additional need to greatly increase the surface area, making this strategy a very appealing feature for developing anode materials with good packing and tap density.^{13,14}

Accordingly, a tailored hydrothermal route is developed to synthesize TiO₂-B nanowires containing rich "lattice voids". It should be noted that tailoring refers to a careful selection of the hydrothermal temperature, NaOH concentration and the calcinations temperature. In contrast to the previous reports^{5,7,9}, a higher hydrothermal temperature at a lower concentration of NaOH is employed to obtain the titanate nanowire precursors. Additional lattice disorder in the structure is induced by lowering the calcination temperature to 300 °C, for which a conventional temperature of 400 °C is needed to obtain crystalline TiO₂-B nanowires.^{5,7,9} Higher tap density is induced by using a relatively higher hydrothermal temperature of 180 °C as opposed to typical reported temperatures of 150 °C, which is favorable for obtaining nanowires with large diameters. The careful selection of the right combination of the three parameters critically influences the electrochemical performance. As a result, the diameter of the nanowires tends to be larger accompanied by loss in surface area but is more than compensated for Li transport by introduction of sufficient micro-voids from a cluster of lattice vacancies within

each of the nanowire. Results show that excellent high-rate discharge performance and high volumetric capacity is available with this modified nanowires.

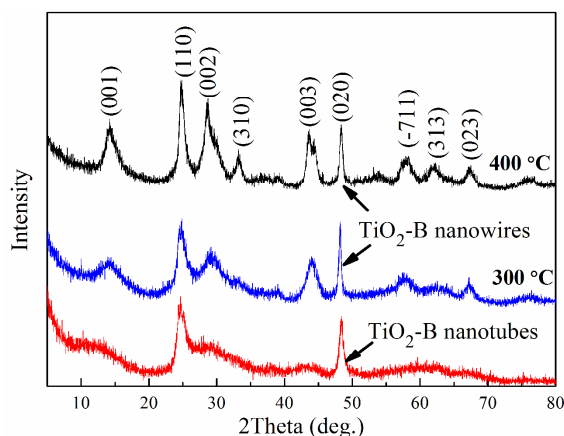


Fig. 1 XRD patterns of as-prepared TiO₂-B nanowires and nanotubes.

Experimental

2.1. Preparation and characterization

Anatase TiO₂ (3.0 g) powder (Analytical) was added to 40 mL of 10 M aqueous solution of NaOH. After sonicating in an ultrasonic bath for 0.5 h, the resulting suspension was transferred to a teflon-lined autoclave and heated to 180 °C for 48 h and then cooled down. The resulting solid gel was recovered and rinsed with distilled water and dilute 0.1 M HCl repeatedly, until a pH of 7 was reached. After drying at 60 °C for at least 2 days, the as-prepared sample was calcined in an oven at 300 °C for 2 h under Ar atmosphere, and TiO₂ nanowires were harvested and characterized. For comparison, TiO₂-B nanowires are prepared via the same process with increasing the thermal treating temperature to 400 °C, and TiO₂-B nanotubes are also prepared according to reference 15.

X-ray diffraction (XRD) was performed on a Rigaku D/max-2500 diffractometer operating in transmission mode with Cu K α radiation. Transmission electron microscopy (TEM) was performed on a FEI Tecnai F20 instrument. Brunauer-Emmett-Teller (BET) measurements were carried out using a NOVA 2000e (Quantachrome) instrument.

2.2 Electrochemical measurements

A 2-electrode cell assembly was used to study the electrochemical behavior of the TiO₂-B electrode. The working electrode was prepared by compressing a mixture of active material (TiO₂-B), acetylene black, and binder (polytetrafluoroethylene, PTFE) in a weight ratio of 75:18:7. The weight of working electrode was around 3 mg with a geometric surface area of 50 mm². A single lithium metal foil was used as both the counter and the reference electrode. LiPF₆ (1 M) dissolved in a mixture of ethylene carbonate (EC), ethyl methyl carbonate (EMC) and dimethyl carbonate (DMC) with a volume ratio of 1:1:1 was used as the electrolyte. Galvanostatic method was employed to measure the electrochemical capacity and cycle life of the working electrode using different charge/discharge current densities successively at 50, 250, 500, 750, 1000, 1500 and 2000 mA g⁻¹ at room temperature with a LAND-CT2001A

instrument. The cut-off potentials for charge and discharge were set at 2.5 and 1.0 V (vs. Li⁺/Li), respectively. Cyclic voltammetry was conducted using a CHI 600A potentiostat at a scan rate of 0.3, 0.5, 0.7 and 1.0 mV s⁻¹, respectively. Current density was calculated taking the geometric area of the working electrode. Electrochemical impedance spectra (EIS) were collected using Zahner IM6e electrochemical workstation. A perturbation of 10mV was applied and data collected under PC control (custom software) from 200 kHz to 10 mHz.

Results and discussion

The XRD patterns of as-prepared TiO₂-B nanowires and nanotubes are given in Fig. 1. All the peaks can be indexed as TiO₂-B phase, with some of the diffraction peaks being broadened.⁵⁻¹² There are no obvious differences between the nanowire prepared at 300 °C and the nanotube XRD patterns. The nanowires obtained at the higher temperature, demonstrate higher crystallinity reflected by the sharper peaks. In order to illustrate the micro-structure of as-prepared samples, TEM images are shown in Fig. 2. As shown in Fig. 2a, the tube-like morphology of TiO₂-B nanotubes is obtained with external diameters of around 10 nm and internal diameters of around 5 nm, in agreement with reported results in the literature.¹⁵ The fringe spacings are ≈ 0.37 nm, consistent with values for bulk TiO₂-B, further confirming the formation of TiO₂-B phase.⁵ For TiO₂-B nanowires prepared at 300 °C, the wire-like morphology can be clearly observed in the lower resolution TEM images (Fig. 2b and c). Compared with previous reports,^{9,10} the TiO₂-B nanowires prepared in this work show a larger diameter around 40-100 nm (as compared with 20-40 nm in references) and can extend up to several micrometers in length containing multitudes of microvoids (≈ 1 nm) along the wire axis (Fig. 2c and d). The larger diameter of nanowires arises from the higher hydrothermal temperature. Different fringe spacings can be simultaneously detected in one single nanowire in the HRTEM image (Fig. 2d), with dimensions of 0.36 nm and 0.64 nm, corresponding to the (110) and (001) planes, respectively of TiO₂-B. It is worth noting that there are irregular voids with interlayer spacing above 1 nm in any single nanowire, and the micro-voids within the lattice can help facilitate faster transport of lithium ions (marked as white box regions in Fig. 2d), thus leading to good rate performance. On increasing the calcination temperature to 400 °C, the nanowire morphology is still retained, accompanied by a small increase in the size for the nanowires as shown in Fig. 2e and 2f. However, the structural micro-voids disappear in the HRTEM image, indicating annealing out of the clusters in nanowire lattice. BET measurements has shown that the surface area of as-prepared nanowires is 18.1 (300 °C) and 16.0 m²/g (400 °C), respectively, indicating that the micro-voids are structural defects formed within the TiO₂-B nanowires,¹⁰ The structural lattice microvoids are expected to allow rapid transport of lithium-ions within each nanowire as compared to TiO₂-B nanowires without such "lattice voids". In contrast, the TiO₂-B nanotubes present a much high surface area value of 320 m²/g and the high rate capability arises from the mesopores rather than the lattice.

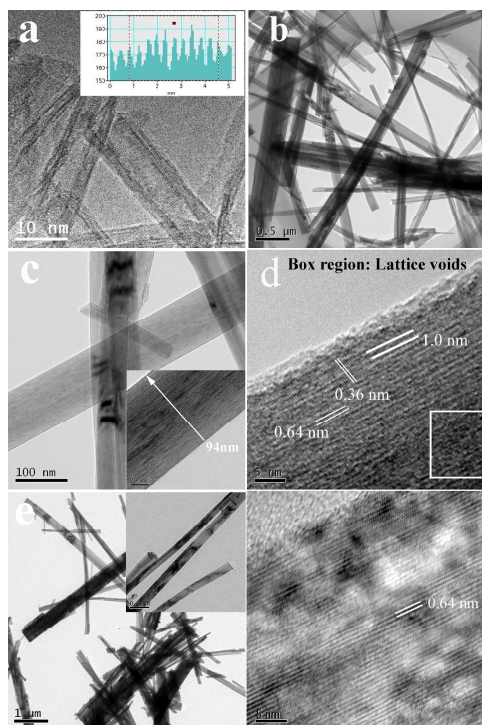


Fig.2 TEM images of TiO₂-B nanotubes (a) and nanowires (b,c,d: 300 °C; e,f: 400 °C) prepared in this work.

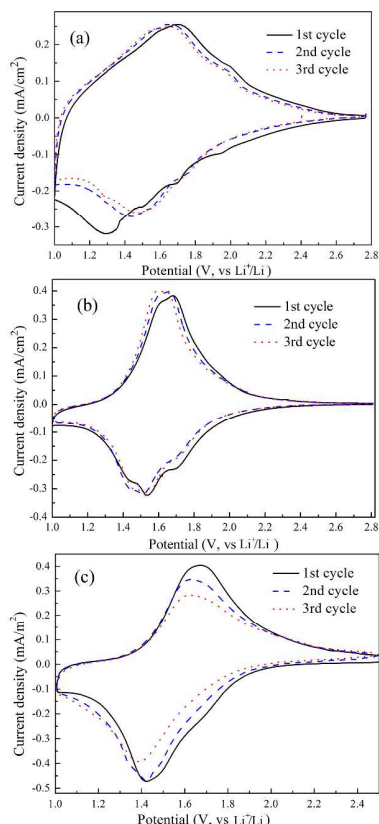


Fig.3 Cyclic voltammograms of the TiO₂-B nanotubes (a) and nanowires (b: 300°C; c: 400°C) at the scan rate of 0.1 mV s⁻¹.

Fig. 3 shows the first several cyclic voltammograms (CVs) for cells with TiO₂-B nanotubes as the working electrode. As shown, only a broad peak appears around 1.3 V during the initial

cathodic process, and an obvious shift can be observed in the following cycles. For TiO₂-B nanowires prepared at 300°C, three cathodic peaks at around 1.69, 1.54 and 1.44 V can be observed, which are known characteristic peaks for TiO₂-B.^{9,16} In the following cycles, as compared to nanotubes, negligible shift of peaks can be observed, indicating better reversibility during cycling. Similar CVs can be seen for the TiO₂-B nanowires prepared at 400 °C. The better reversibility for nanowires can be attributed to its more stable solid structure as compared to hollow nanotubes. Furthermore, as compared the TiO₂-B nanowires prepared at 400 °C ($\Delta E_p=245$ mV), TiO₂-B nanowires prepared at 300 °C ($\Delta E_p=100$ mV) demonstrates an obvious smaller potential gap, in consistent with the previous report, indicating more facile mass transport of both electrolyte through the electrode as well as enhanced Li⁺ diffusion result from the "lattice voids".¹⁷

To investigate the high rate discharge/charge and the cycle performance of the TiO₂-B nanowires and nanotubes, the variation of discharge capacity with cycles at increasing current densities from 50 to 2000 mA g⁻¹ applied successively followed by a return to 50 mA g⁻¹ after 80 cycles is shown in Fig. 4. As shown in Fig. 4a, both samples demonstrate good cycle performance. When the current density is below 1500 mA g⁻¹, the TiO₂-B nanotubes demonstrate a higher discharge capacity than nanowires. However, when the current density increases to 2000 mA g⁻¹, the nanowires present discharge capacity at 129.0 mAh g⁻¹ after 80 cycles, which is higher than TiO₂-B nanotubes. Results using TiO₂-B nanowires as anode are reported to show capacity of 100 mAh g⁻¹ at the current density of 2000 mA g⁻¹ after 80 cycles.⁹ Thus the lower BET surface area TiO₂-B nanowires as prepared in this work show obvious rate advantages over both nanotubes and nanowires with much smaller diameters and much higher surface areas.⁹ The advantages of such 'lattice-voids' can be further illustrated as compared to TiO₂-B nanowires prepared at 400 °C. It demonstrates a low initial discharge capacity at 158.4 mAh g⁻¹, and the capacity rapidly decrease to 83 mAh g⁻¹ after 20 cycles at the current density of 50 mAh g⁻¹. When the current density is increased to 2000 mAh g⁻¹, TiO₂-B nanowires prepared at 400 °C is difficult to charge. Such a poor electrochemical performance mainly arise the disappearance of 'lattice voids'. Furthermore, after the 80th cycle using the successively increasing current densities, the present working electrode made of nanowires still retained a discharge capacity of 225.1 mAh g⁻¹ for another 20 cycles when the current density was returned to 50 mA g⁻¹. Therefore, the as-prepared TiO₂-B nanowires can endure significant changes of low or high current densities and yet retain good stability upon cycling, and this is advantageous for abuse tolerance of lithium-ion batteries with the high power and long cycle life.¹⁸ Fig. 4b is the corresponding discharge-charge curves of TiO₂-B nanowires and nanotubes. Different discharge curves can be observed for the nanowires and nanotubes, for which TiO₂-B nanowires demonstrate a more obvious sloping plateau between 1.8-1.3V. And when the current density is enhanced to 2000mA g⁻¹, the sloping plateau is still retained, indicating a fast kinetic process for the nanowires. At a current density of 50 mA g⁻¹, the TiO₂-B nanotubes demonstrate an ultra high initial discharge capacity of around 437.5 mAh g⁻¹, but also a high irreversible capacity of about 112 mAh g⁻¹. For

TiO₂-B nanowires, the initial discharge capacity is about 263.8 mAh g⁻¹, lower than that of the nanotubes, but the ratio of reversible capacity can reach up to 90%. The large irreversible capacity of nanotubes may relate to its high surface area and the resulting parasitic surface reactions.⁸ Also, it can be seen that the TiO₂-B nanowires show a much better cycle performance as compared to the nanotubes, and this can be clearly revealed by the figure of capacity retention in Fig. 4c. As presented, the capacity retention of the TiO₂-B nanowires is 68% for the discharge capacity between 250 and 2000 mA g⁻¹, while it is just about 51.5% for TiO₂-B nanotubes. Additionally, the obtained TiO₂-B nanowires demonstrate a significant higher tap density as compared to nanotubes shown in the inset figure, which is about 100% higher after tapping within a graduated cylinder under similar conditions. . By calculating from the tap density and discharge capacity at various current densities, the ratio of volumetric capacity is given in Fig. 4d. As shown, the obtained TiO₂-B nanowires demonstrate a much higher volumetric capacity as compared TiO₂-B nanotubes. Especially, such advantages is more obvious at high current density of 2000 mA g⁻¹, and the ratio can reach up to twice the value. The high volumetric capacity of the TiO₂-B nanowires will translate into a high volume energy density, and making the electrode more appealing as compared to nanotubes, which is key parameter in the practical applications.

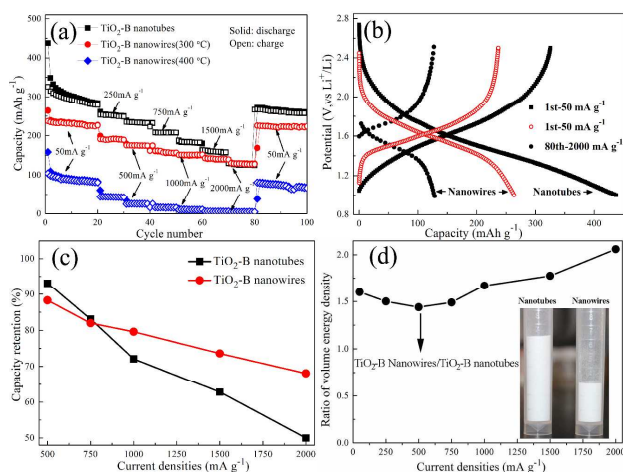


Fig.4 (a) Cycle curves of TiO₂-B nanowires and nanotubes at variation current densities; (b) Discharge-charge curves of TiO₂-B nanotubes and nanowires; (c) Capacity retention at various current densities as compared to that at the current density of 250 mA g⁻¹. (d) The ratio of volumetric capacity by comparing the TiO₂-B nanowires and nanotubes at various current densities. Inset is the volume comparison of TiO₂-B nanowires and nanotubes after same treatment (1g, respectively).

To illustrate the reason of the different rate performance between nanowires and nanotubes, EIS tests were conducted, and the results are given in Fig. 5. Both Nyquist plots consist of one depressed semicircle at high frequencies and a straight line at low frequencies before discharge. The diameter of high frequencies semicircle refers to the charge transfer resistance, relating to the electrochemical reaction at the electrode-electrolyte interface.^{19,20} As seen, the charge transfer resistance of the TiO₂-B nanotubes is significantly smaller than that TiO₂-B nanowires. For the EIS test before discharge, the charge transfer resistance mainly relates to

the wettability between the electrolyte and electrode, and such a decrease of charge transfer resistance of nanotubes can be attributed to its developed porous structure, thus leading to a high initial discharge capacity. After discharging to 1.0 V, two semicircles can be observed for TiO₂-B nanotubes, and the additional semicircle can be attributed to the solid electrolyte interphase (SEI), resulting from the high surface area and side reactions.^{8,19,20} The generation of SEI will lead to a low coulombic efficiency during initial cycles and obviously increase the charge-transfer resistance. For TiO₂-B nanowires, there are no obvious changes in the Nyquist plot after discharging, with a negligible increase in charge transfer resistance is observed. To further illustrate the reasons for the high rate performance of TiO₂-B nanowires, the Li-ion diffusion coefficient of TiO₂-B nanotubes and nanowires is compared by calculating the data from the EIS results. The change of Li-ion diffusion coefficient D_{Li} in the compound can be calculated from the low frequency linear Warburg regions according to the equation:²²

$$D_{Li} = 1/2[(V_m/FA\sigma_w) \cdot d_E/d_x]^2$$

where V_m is the molar volume of TiO₂, F is the Faraday constant, A is the total contact area between the electrolyte and the electrode, and σ_w is the Warburg coefficient which can be obtained from the plotting Z_{Re} against $\omega^{-1/2}$ in the low frequency region in the Nyquist EIS spectra presented in Fig. 5a and 5b. As shown in Fig. 5c, the Warburg coefficient of nanotubes and nanowires is 8.1749 and 36.496, respectively. The d_E/d_x can be obtained from the slopes of the discharge curve in Fig. 5d, and the slopes of the discharge for nanotubes and nanowires at the potential of 1.0V are -0.88 and -3.62, respectively. Obviously, the obtained nanowires with “lattice voids” show a similar Li-ion diffusion coefficient as nanotubes, and this can offer a suitable explanation for the excellent rate performance of TiO₂-B nanowires, consistent with the results of CVs discussed above.

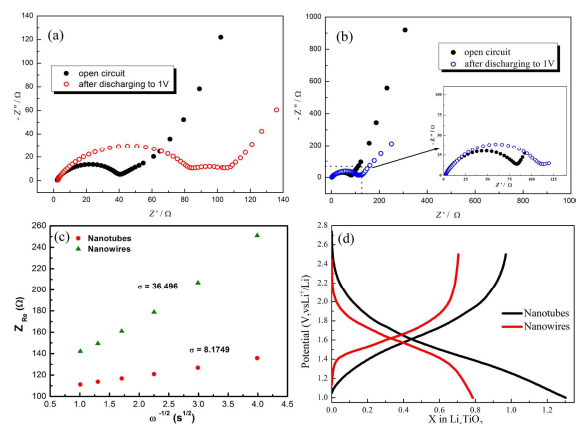


Fig.5 Nyquist plots of TiO₂-B nanotubes (a) and nanowires (b, 300 °C) at open-circuit voltage before cycling and after discharging to 1.0 V. (c) Z_{Re} vs $\omega^{-1/2}$ plots in the low frequency region obtained from EIS measurements. (d) Discharge-charge curve at a current density of 50 mA g⁻¹.

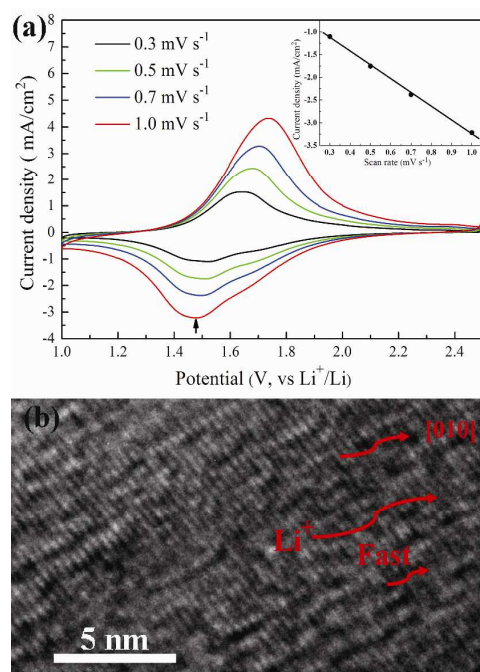


Fig.6 (a) Cyclic voltammograms of the TiO₂-B nanowires at different scan rates after initial three cycles at a scan rate of 0.1 mV s⁻¹ and the insertion is the relationship between the peak current and the scan rate; (b) schematic illustration of Li-intercalation into TiO₂-B nanowires.

As compared to TiO₂-B nanowires reported before, the obtained nanowires in this work show a larger diameter with lower surface area, and yet has shown an enhanced high rate capability. Thus we have shown that it is possible to engineer lattice defects in the form of vacancy clusters that can help produce improved electrode performance. The defects in structure, of the TiO₂-B nanowires are depicted as structural micro-voids of around 1 nm dimension longitudinally distributed within each nanowire. This morphology is highly conducive to good high-rate performance as an anode. In order to shed further light on the high rate discharge nature of TiO₂-B, cyclic voltammetry experiments at different scan rates were conducted and results are displayed in Fig. 6a. At a scan rate of 1 mV s⁻¹, the typical S-peaks disappear and a pair of broad cathodic/anodic peaks appears around 1.48 and 1.72V, corresponding to Li insertion and Li removal. It is well-known that the relation between peak currents and scan rates indicate the different electrochemical reaction characteristics.^{23,24} Square root dependence of peak current with respect to the scan rate is associated with solid phase diffusion-controlled processes in the bulk, while a linear relationship between the peak current and scan rates indicates a pseudocapacitive process.²³⁻²⁶ As shown, lithium-ion storage in TiO₂-B nanowires is dominated by pseudocapacitive faradaic currents at the scan rates investigated in this work. Pseudocapacitance is a surface-confined charge transfer process and thus corresponds to a high rate lithium storage process. The dominant faradic pseudocapacitive effect is favorable for enhancing the high rate discharge performance of the TiO₂-B nanowires, and a schematic presentation is given in Fig. 6b. For TiO₂-B nanowires, they will grow along the b-axis, and produce abundant parallel channels perpendicular to the (010) face. The transfer of lithium-ion is fast through the channels, and the

surface transfer of lithium will become the rate-determining process, leading to the pseudocapacitive effect.²³⁻²⁶ The generation of micro-voids within each nanowires can produce a more defective structure to both accelerate the lithium-ion transfer through the surface and the bulk material, confirmed by the EIS and CV measurements. Such a partial disordered structure in TiO₂-B nanowires can further enhance the pseudocapacitive contributions in lithium storage, and thus produce a better rate performance.

Another very significant benefit is derived from the higher tap density obtained for the TiO₂-B nanowires (300 °C) in comparison with the nanotubes. As shown in Fig. 4, the nanowires (300 °C) pack twice as efficiently as the nanotubes thus greatly helping increase the relative volumetric energy density at all current densities from 50-2000 mA g⁻¹. Thus a controlled nanosize strategy combined with the introduction of lattice micro-voids is an excellent approach for simultaneously achieving high rate capability and high volumetric energy density in a Li-ion battery. Volumetric capacity is a critical parameter in battery applications where maximal use of space is important.

Conclusions

TiO₂-B nanowires were successfully prepared from anatase powder by employing a hydrothermal process at 180 °C followed by acid washing ion-exchange and calcination at 300 °C. As a result of the relatively higher hydrothermal temperature, the nanowires have relatively larger diameters and lower surface area but excellent tap densities. The lower calcinations temperature can confer lattice micro-voids which can compensate for the loss of BET surface area and the associated mesopores. The discharge capacity of as-prepared sample is found to be 226.8 mAh g⁻¹ after the 20th cycle at the charge/discharge current density 50 mA g⁻¹, and it remained still impressive at 129.0 mAh g⁻¹ when the current density is increased to 2000 mA g⁻¹ in successive steps through various current densities. Good rate performance is attributed to its unique micro-void structure within each nanowire while the increased tap density offers high volumetric capacity. The strategy of modifying the crystal structure offers novel insights into developing high performance electrode materials, and the application in other electrode materials are currently being investigated.

Acknowledgements

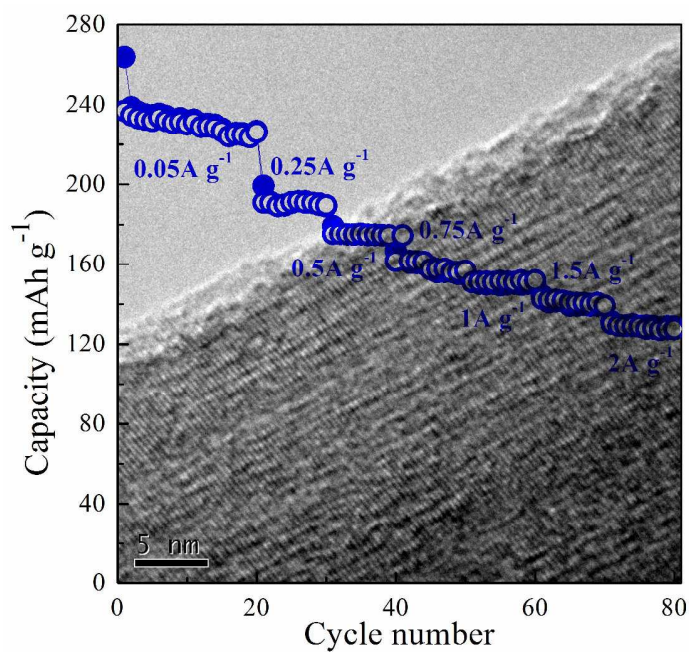
This work has been supported by the Chinese National Science Funds (No. 51202094); the Priority Academic Program Development of Jiangsu Higher Education Institutions; the Natural Science Foundation (No. 12KJB150010) of Jiangsu Education Committee of China. Kai Xi thanks the Cambridge Overseas Trust.

Notes and references

- ^a School of Chemistry and Chemical Engineering, and Jiangsu Key Laboratory of Green Synthetic Chemistry for Functional Materials, Jiangsu Normal University, Xuzhou, Jiangsu 221116, China, Email: laichao@jsnu.edu.cn;
- ^b Department of Materials Science and Metallurgy, University of Cambridge, Cambridge, CB2 3QZ, UK. Email: kx210@cam.ac.uk

- 1 J. B. Goodenough and Y. Kim, *Chem. Mater.*, 2010, **22**, 587.
- 2 J. Liu, J.-G. Zhang, Z. Yang, J. P. Lemmon, C. Imhoff, G. L. Graff, L. Li, J. Hu, C. Wang, J. Xiao, G. Xia, V. V. Viswanathan, S. Baskaran, V. Sprenkle, X. Li, Y. Shao and B. Schwenzer, *Adv. Funct. Mater.* 2012, **23**, 929.
- 3 G.X. Zhao, T. Wen, C.L. Chen and X.K. Wang, *RSC Adv.* 2012, **2**, 9286.
- 4 D. Deng, M.G. Kim, J.Y. Lee and J. Cho, *Energy Environ. Sci.* 2009, **2**, 818.
- 5 A.R. Armstrong, G. Armstrong, J. Canales and P.G. Bruce, *Angew. Chem. Int. Ed.* 2004, **43**, 2286.
- 6 Q.J. Li, J.W. Zhang, B.B. Liu, M. Li, R. Liu, X.L. Li, H.L. Ma, S.D. Yu, L. Wang, Y.G. Zou, Z.P. Li, B. Zou, T. Cui and G.T. Zou, *Inorg. Chem.* 2008, **47**, 9870.
- 7 G. Armstrong, A.R. Armstrong, J. Canales and P.G. Bruce, *Electrochem. Solid-state Lett.* 2006, **9**, A139.
- 8 S. Brutti, V. Gentili, H. Menard, B. Scrosati and P.G. Bruce, *Adv. Energy Mater.* 2012, **2**, 322.
- 9 A.R. Armstrong, G. Armstrong, J. Canales and P.G. Bruce, *J. Power Sources* 2005, **146**, 501.
- 10 J.M. Li, W. Wan, H.H. Zhou, J.J. Li and D.S. Xu, *Chem. Commun.* 2011, **47**, 3439.
- 11 V. Etacheri, Y. Kuo, A.V. Ven and B.M. Bartlett, *J. Mater. Chem. A*, 2013, **1**, 12028.
- 12 Z.Y. Guo, X.L. Dong, D.D. Zhou, Y.J. Du, Y.G. Wang and Y.Y. Xia, *RSC Adv.*, 2013, **3**, 3352.
- 13 H.T. Fang, M. Liu, D.W. Wang, T. Sun, D.S. Guan, F. Li, J.G. Zhou, T.K. Sham and H.M. Cheng, *Nanotechnology* 2009, **20**, 225701.
- 14 V. Augustyn, J. Come, M. A. Lowe, J.W. Kim, P.L. Taberna, S.H. Tolbert, H.D. Abruña, P. Simon and B. Dunn, *Nat. Mater.* 2013, **12**, 518.
- 15 J. Qu, Q.D. Wu, Y.R. Ren, Z. Su, C. Lai and J.N. Ding, *Chem. Asian J.* 2012, **7**, 2516.
- 16 M. Zukalov, M. Kalbc, L. Kavan, I. Exnar and M. Graetzel, *Chem. Mater.* 2005, **17**, 1248.
- 17 A.G. Dylla, J.A. Lee and Keith J. Stevenson, *Langmuir* 2012, **28**, 2897.
- 18 C. Lai, H.Z. Zhang and X.P. Gao, *J. Power sources* 2011, **196**, 4735.
- 19 J.Y. Shen, H. Wang, Y. Zhou, N.Q. Ye, G.B. Li and L.J. Wang, *RSC Adv.* 2012, **2**, 9173.
- 20 J.M. Zheng, M. Gu, H.H. Chen, P. Meduri, M.H. Engelhard, J.G. Zhang, J. Liu and J. Xiao, *J. Mater. Chem. A* 2013, **1**, 8464.
- 21 H.L. Guo and Q.M. Gao, *J. Power Sources* 2009, **186**, 551.
- 22 Y.G. Wang, H.M. Liu, K.X. Wang, H. Eiji, Y.R. Wang and H.S. Zhou, *J. Mater. Chem.* 2009, **19**, 6789.
- 23 J. Wang, J. Polleux, J. Lim and B. Dunn, *J. Phys. Chem. C* 2007, **111**, 14925.
- 24 A.G. Dylla, G. Henkelman and K.J. Stevenson, *Acc. Chem. Res.* 2013, **46**, 1104.
- 25 D. Panduwinata and J.D. Gale, *J. Mater. Chem.* 2009, **19**, 3931.
- 26 V. Augustyn, J. Come, M.A. Lowe, J. Kim, P.-L. Taberna, S.H. Tolbert, H.D. Abruña, P. Simon and B. Dunn, *Nat. Mater.* 2013, **12**, 518.

Graphical Abstracts



Enhanced high-rate performance of TiO₂-B nanowires can be achieved by introducing “lattice voids” to produce a partial disorder structure. The obtained TiO₂-B nanowires can show the same excellent rate capability as TiO₂-B nanotubes, but a much higher volumetric capacity and better capacity retention.